



ELSEVIER

Contents lists available at [ScienceDirect](#)

## Journal of Sound and Vibration

journal homepage: [www.elsevier.com/locate/jsvi](http://www.elsevier.com/locate/jsvi)

## Footbridge system identification using wireless inertial measurement units for force and response measurements

James Mark William Brownjohn<sup>a,\*</sup>, Mateusz Bocian<sup>b</sup>, David Hester<sup>c</sup>,  
Antonino Quattrone<sup>d</sup>, William Hudson<sup>a</sup>, Daniel Moore<sup>a</sup>, Sushma Goh<sup>e</sup>,  
Meng Sun Lim<sup>f</sup>

<sup>a</sup> University of Exeter, UK,<sup>b</sup> University of Leicester, UK<sup>c</sup> Queens's University, Belfast, UK<sup>d</sup> Politecnico di Torino, Italy<sup>e</sup> Projects and Facilities Management Group, National Gallery, Singapore<sup>f</sup> CPG Consultants, Pte Ltd, Singapore

## ARTICLE INFO

*Article history:*

Received 6 March 2016

Received in revised form

1 August 2016

Accepted 3 August 2016

Handling Editor: J. Macdonald

*Keywords:*

Footbridge vibration

Human jumping

Modal mass identification

Wireless sensor

## ABSTRACT

With the main focus on safety, design of structures for vibration serviceability is often overlooked or mismanaged, resulting in some high profile structures failing publicly to perform adequately under human dynamic loading due to walking, running or jumping. A standard tool to inform better design, prove fitness for purpose before entering service and design retrofits is modal testing, a procedure that typically involves acceleration measurements using an array of wired sensors and force generation using a mechanical shaker. A critical but often overlooked aspect is using input (force) to output (response) relationships to enable estimation of modal mass, which is a key parameter directly controlling vibration levels in service.

This paper describes the use of wireless inertial measurement units (IMUs), designed for biomechanics motion capture applications, for the modal testing of a 109 m footbridge. IMUs were first used for an output-only vibration survey to identify mode frequencies, shapes and damping ratios, then for simultaneous measurement of body accelerations of a human subject jumping to excite specific vibrations modes and build up bridge deck accelerations at the jumping location. Using the mode shapes and the vertical acceleration data from a suitable body landmark scaled by body mass, thus providing jumping force data, it was possible to create frequency response functions and estimate modal masses.

The modal mass estimates for this bridge were checked against estimates obtained using an instrumented hammer and known mass distributions, showing consistency among the experimental estimates. Finally, the method was used in an applied research application on a short span footbridge where the benefits of logistical and operational simplicity afforded by the highly portable and easy to use IMUs proved extremely useful for an efficient evaluation of vibration serviceability, including estimation of modal masses.

© 2016 The Authors. Published by Elsevier Ltd. This is an open access article under the CC BY license (<http://creativecommons.org/licenses/by/4.0/>).

\* Correspondence to: CEMPS, University of Exeter, Harrison Building, Exeter EX4 4QF, UK.

E-mail addresses: [J.Brownjohn@exeter.ac.uk](mailto:J.Brownjohn@exeter.ac.uk) (J.M. William Brownjohn), [m.bocian@leicester.ac.uk](mailto:m.bocian@leicester.ac.uk) (M. Bocian), [d.hester@qub.ac.uk](mailto:d.hester@qub.ac.uk) (D. Hester), [antonino.quattrone@polito.it](mailto:antonino.quattrone@polito.it) (A. Quattrone), [w.hudson@elliottwood.co.uk](mailto:w.hudson@elliottwood.co.uk) (W. Hudson), [dm353@hotmail.com](mailto:dm353@hotmail.com) (D. Moore), [sushma.goh@nationalgallery.sg](mailto:sushma.goh@nationalgallery.sg) (S. Goh), [Leong.Meng.Sun@cpccorp.com.sg](mailto:Leong.Meng.Sun@cpccorp.com.sg) (L.M. Sun).

<http://dx.doi.org/10.1016/j.jsv.2016.08.008>

0022-460X/© 2016 The Authors. Published by Elsevier Ltd. This is an open access article under the CC BY license (<http://creativecommons.org/licenses/by/4.0/>).

## 1. Introduction and objectives

With the main focus on safety, design of structures for vibration serviceability is often overlooked or mismanaged, resulting in some classic and public failures [1,2] to perform adequately under human dynamic loads due to walking, running or jumping.

Designing for, assessing and improving vibration serviceability of footbridges for human dynamic loading requires reliable estimates of modal parameters, which may be obtained from numerical simulation (finite element modelling) or from full-scale testing (modal testing and system identification). In either case the ensuing performance simulations will assume bridge behaviour in the linear range so that modal responses can be treated individually and then summed directly in either time or frequency domain.

The numerical modelling route is the only option for a footbridge yet to be built, but for a structure being retrofitted (e.g. with a tuned mass damper) or that has been completed but not yet opened to the public, the most reliable values of modal parameters are recovered by in-situ testing. This approach was adopted for vibration serviceability assessment of Singapore's Helix Bridge [3] where modal parameters from a full-scale test using a pair of shakers and an array of wired accelerometers were used to create a modal model. In-house simulation software was then used to simulate and assess response in line with relevant guidance.

The Helix Bridge modal test was a major exercise involving costly air-freighting of 125 kg of sensors and cabling and loan of two heavy shakers from 1<sup>st</sup> author's local contacts. Considering the logistical complexity of the testing exercise and the comprehensive level of performance data provided begs the question: what is the logistically simplest testing programme that can be used to provide just enough information for required performance assessment?

Hence the objective of the research described here was to evaluate:

- 1) The capability of lightweight portable wireless MEMS accelerometers for synchronous acceleration measurements at multiple locations on a footbridge of sufficient quality for reliable operational modal analysis;
- 2) The capability of the same sensors to allow indirect estimation of ground reaction forces (GRFs) during jumping, as a means of exciting response in specific footbridge vibration modes;
- 3) The feasibility of using the GRF (input) and footbridge acceleration (output) as a low cost method to generate frequency response functions of sufficient quality to recover all modal parameters including modal mass.

The study considers only vertical vibration modes and does not directly address human-structure interaction. Two footbridges are chosen for the study, but as the objectives are purely to demonstrate capability for full modal parameter identification, neither their serviceability nor features of their dynamic behaviour or any human-structure interaction are discussed. However, it is believed the methodology opens up new possibilities for such studies through in-situ field testing.

### 1.1. Modal testing of footbridges

A variety of modal testing methods are available for footbridges and there is extensive literature [4–7] on case studies primarily relating to vibration serviceability for both vertical and lateral vibrations.

Footbridges, particularly those requiring investigation are often lightweight, their natural frequencies tend to be below 5 Hz and damping ratios can be below 1 percent. As such, they can be very lively under the exact type of loading for which they are designed.

For a 'well behaved' footbridge acting as a simply supported beam and having well separated modes with shapes resembling sine waves, identification of natural frequencies and damping ratios can be very simple: a single accelerometer and a time domain system identification procedures such as the logarithmic decrement method. For more complex structures with closely spaced vibration modes and irregular mode shapes more elaborate instrumentation involving large numbers of measurement points and sensors along with sophisticated system identification procedures including operational modal analysis are needed [7,8].

### 1.2. Estimating modal mass

The requirement for a measurable and controllable mechanical excitation and difficulties with accurate estimation mean that modal mass is seldom reported from footbridge modal tests. However, if the modal test data are to be used via a modal model to simulate in-service performance and develop vibration mitigation strategies including retrofit, a reliable modal mass estimate is vital. Direct experimental estimation of modal mass requires in-situ measurement of excitation forces, applied via an instrumented hammer [7], drop-weight [7] or shaker [3]. These devices have practical limitations; instrumented hammers are highly portable and need only battery power, but testing requires careful adjustment of signal to noise ratios to avoid overloading (nearby) sensors while sharing enough energy among all the modes engaged by a single impulse. A well-designed drop-weight with deceleration pulse shaped to focus force in the low frequency range should perform better than a hammer but is far less portable. Shaker testing is the ideal solution but shakers are expensive, heavy, and require powerful electrical supplies and synchronised signal generation.

Nomenclature			
AVT	ambient vibration test	$\beta$	parameter defining the rate of decay of exponential window
C7	7th cervical vertebra (location for IMU)	$\zeta_n$	damping ratio of mode $n$
CHS	circular hollow section	$\zeta_{n,\text{add}}$	added damping ratio due to the application of exponential window for mode $n$
CSD	cross-spectral density	$\omega$	circular frequency
DLF	magnitude of harmonic force component expressed as a fraction of the weight of the walker	$\omega_n$	circular natural frequency
ERA	eigensystem realisation algorithm	$\psi_j$	modal ordinate at point $j$
FFT	fast (discrete) Fourier transform	$A$	modal constant
FRF	frequency response function	$D$	diameter of frequency response function circle as Nyquist plot
GRF	ground reaction force	$F_k(\omega)$	frequency domain forcing function at point $k$
HPB	half-power band	$T$	duration of transient event
IMU	inertial measurement unit	$W$	exponential time window
IRF	impulse response function	$X_j(\omega)$	frequency domain displacement response at point $k$
LB	lower back (location for IMU)	$df$	inverse of $T$
LCS	local coordinate system	$f_n$	natural frequency
MEMS	micro-electrical-mechanical system	$i$	irrational number ( $=\sqrt{-1}$ )
RHS	rectangular hollow section	$j, k$	points along the bridge
RSA	rolled steel angle	$m_j$	mass of the bridge assumed lumped at point $j$
S	sternum (location for IMU)	$m_n$	modal mass of mode $n$
SHS	square hollow section	$n$	mode identifier
TP	test point (for vibration measurements and mode shape ordinates)	$n_{\text{HPB}}$	number of frequency lines between points where frequency response function is 70 per cent of maximum value
UB	Universal beam	$t$	time
WCS	world coordinate systems		
<i>List of symbols</i>			
$\alpha(\omega)$	frequency response function		

Using humans jumping or walking to generate response is somehow ideal and is a practice widely used in footbridge dynamic testing. However, while wearing accelerometers to track human body accelerations is far from new [e.g. 9], there appears to be no example of their use for in-situ simultaneous measurements of both pedestrian forcing and footbridge response enabling reliable estimation of modal mass. This would be a highly efficient approach because the forces involved and response generated are of the same order as would be experienced in normal footbridge service and no artificial excitation would be required. So far this has not been feasible, hence alternative methods for modal mass estimation have been devised that are based on laboratory-calibrated jumping or walking, but being indirect they lack the reliability of direct measurement of in-situ force or some proxy [10]. A logical development would be direct measurement of the in-situ human forces e.g. using a force plate, but these instruments are not well suited to routine field use, being heavy and cumbersome and requiring proprietary cables with limited length and connections along with their own power and signal conditioning.

### 1.3. Indirect measurement of in-situ ground reaction forces

Since a previous study on indirect modal mass estimation [10] there have been significant advances in methods and tools for measurements of human dynamic loads such as jumping forces. For example it is now recognised [11] that jumping ground reaction forces (GRFs) obtained by summing 'inertia forces' of body parts agree very well with direct force plate measurements. Body segment masses are obtained from the (live) jumper with mass distributions from cadaver (anthropometric) data. Accelerations are obtained by double-differentiation of displacements obtained using optical motion capture systems with active or passive markers.

While optics-based motion capture avoids the need for jumping/walking on an instrumented surface it is effectively restricted to laboratory use: the sophisticated cameras are expensive and delicate, require careful placement within a range of a few metres of the marker-clad human and are highly sensitive to lighting conditions, including infra-red radiation within sunlight spectrum.

An obvious alternative to optics-based motion capture is inertial measurement units (IMUs) used by biomechanics and sports science researchers [12]. These free the experiment from laboratory constraints and provide acceleration data directly. The potential limitations relate to:



**Fig. 1.** APDM Opal™ inertial measurement unit showing local coordinate system (LCS) axes; +z is vertical, upwards. A one-pound coin is shown for size reference.

- precise synchronisation of wireless sensors in the open space environment of a footbridge;
- the need to convert from local coordinate systems (LCS) oriented with the IMU to the world coordinate system (WCS) oriented with the structure;
- effective representation of body mass and its movement using a small number of IMUs, maybe even limiting to a single unit for the pedestrian.

## 2. Deployment of wireless inertial measurement units (IMUs)

This paper describes an application of a particular type of wireless IMU, the APDM Opal™, (Fig. 1) not only for in-situ GRF recovery but also for modal testing. While testing the viability of these IMUs to capture both timing and GRF data in a study of pedestrian synchronisation on footbridges around Exeter in 2015 [13], it was found that they are also well suited for measuring the relatively strong human-induced responses of this class of structure. This discovery led to their deployment for complete system identification of one of these footbridges, and subsequently for a new footbridge in Singapore, as described in this paper.

A set of six Opal™ IMUs is used with a wireless access point or a docking station connected to a host computer (PC). Each IMU, based on Micro-Electro-Mechanical System (MEMS) technology, incorporates a magnetometer to sense orientation with respect to Earth's magnetic field, a triaxial accelerometer and a triaxial gyroscope. IMU resources managed by a microcontroller include wireless communication and on-board flash memory. Information from the magnetometer and gyroscopes are particularly important for body-worn IMUs as the data allow the accelerations to be resolved from IMU local coordinate system (LCS) to world coordinate system (WCS), providing a purely vertical acceleration signal, uncontaminated by lateral movements.

The accelerometers have noise floor of  $120 \mu\text{g}/\sqrt{\text{Hz}}$  i.e.  $1200 \mu\text{g}$  in 0 to 100 Hz bandwidth. With 14-bits available in the analogue to digital converter, for the  $\pm 2 \text{ g}$  and  $\pm 6 \text{ g}$  ranges offered, corresponding resolution is  $240 \mu\text{g}$  and  $730 \mu\text{g}$ . Such sensitivity is adequate for studying behaviour of footbridges but Opals™ are not suitable for studying low level vibrations in, for example, sway of high rise buildings. For all the measurements described herein the sample rate was set to 128 Hz per channel.

Opal™ IMUs are synchronised in two ways. For monitors working in a *synchronised streaming* mode, the wireless access point transmits a synchronisation trigger to the set of IMUs, and data packets from each IMU are time-stamped according to an internal clock of the unit, adjusted according to the acquired master time. This mode is suitable for close range use. *Synchronised logging* mode is used when wireless communication between the access point and IMUs cannot be maintained, and the units establish mesh synchronisation. In this mode no master time is assumed and global synchronisation is achieved collaboratively utilising probabilistic models applied to time information from internal clocks. Data are downloaded using the docking station. In this mode the IMUs can operate tens of metres apart.

The IMUs were designed specifically for motion capture, whereas there are solutions available for cable-free measurement of structural acceleration, including bespoke wireless sensors such as the Imote2 device [14–16] and autonomous seismometers such as GeoSIG recorders [17]. Experience with these devices indicates that they would be unsuitable for the application described here.

## 3. Synchronisation project and Baker Bridge

This paper initially focuses on application of IMUs to one particular bridge as part of a research project on 'Human Synchronisation Effects in Structural Dynamics'. The application was a research sub-project carried out by a group of eight final year undergraduate students at the University of Exeter in 2015 and whose aim was to study pedestrian synchronisation among footbridge users and with the vibrating structure. The footbridge chosen for the project was Baker Bridge ( $50^\circ 42' 38.35'' \text{N}$   $3^\circ 28' 13.30'' \text{W}$ ), see Fig. 2, a 109 m cable-stayed bridge crossing the busy A379 dual-carriageway in Exeter. The Bridge provides cycle and pedestrian access to Sandy Park Stadium, the home ground of Exeter Chiefs Rugby Club. The primary function of the bridge is to ease road traffic congestion on match days, when the bridge experiences heavy pedestrian traffic and demonstrates a lively dynamic response.

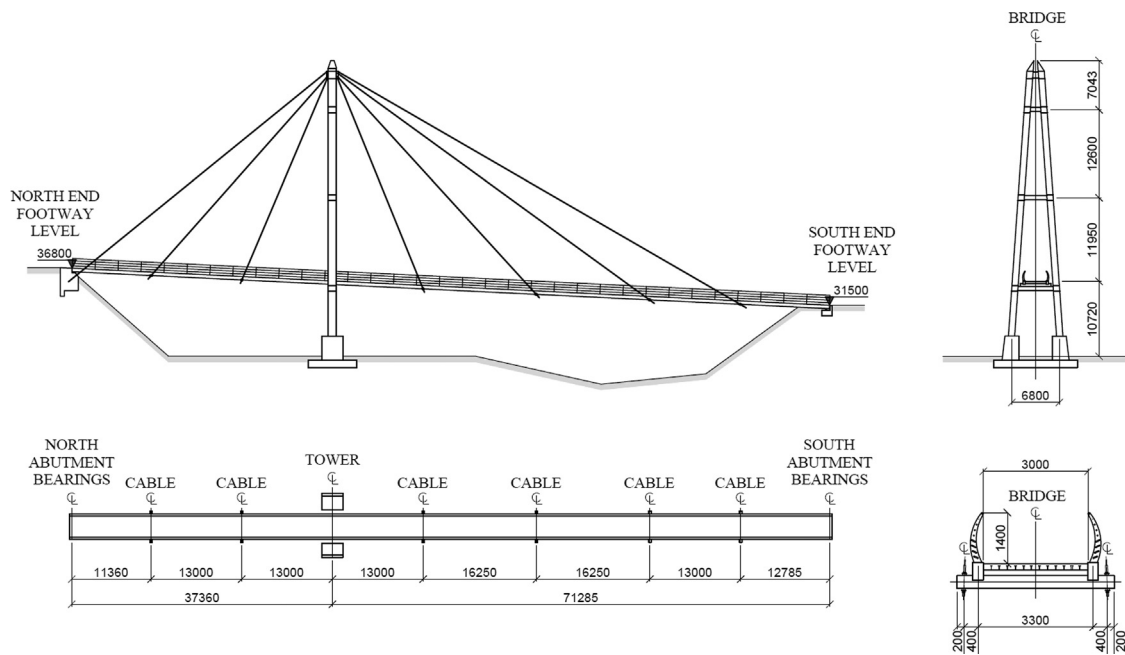


Fig. 2. Baker Bridge; information from as-built drawings.

The bridge comprises a single A-shaped 42 m tower supporting the deck via seven pairs of cables secured to the top of the tower; four cable pairs to a long front span on the (South) stadium side, two cable pairs to a short back span on the North side and one pair to a counterbalancing concrete mass at the north abutment. The counterbalance cables are 65 mm diameter, the remaining 12 are 25 mm, 30 mm and 35 mm, going with cable length. The twin uprights of the tower are steel rectangular hollow section (RHS) 1200 × 600 mm, while square hollow section (SHS) are used for the three crossbeams: two above deck, the other directly below the deck and providing vertical support to the deck while restraining lateral motion. Massive reinforced concrete bases support the tower via anchor plates, protecting against vehicle collision.

The deck comprises two 109 m Grade 50 steel 500x300 × 16 mm RHS longitudinal beams with transverse 150x150 × 5 mm SHS beams at 3.1 m centres. 100x100 × 8 mm rolled steel angle (RSA) sections welded to the RHS beams provide support for the 120 mm in-situ reinforced concrete walkway, which is also secured to the SHS beams by  $\phi 19 \times 74$  mm shear studs at 150 mm centres. The six cables are secured to 324 × 16 mm circular hollow section (CHS) crossbeams which support the longitudinal beams. Parapets are bolted to the RHS beam via curved, 15 mm-thick steel plate uprights at 2.5 m centres. The estimated total mass of the bridge is 150 t.

Given the reported lively behaviour, Baker Bridge was checked by (metronome) prompted walking, to provide crude estimates of a number of natural frequencies in the 1–2 Hz range. Devon County Council granted permission to test and provided a set of drawings, and vibration measurements and pedestrian tests were carried out in early 2015 by the students and researchers. All tests involving human subjects were approved by the College of Engineering, Mathematics and Physical Sciences Research Ethics Committee at the University of Exeter.

#### 4. Vibration measurements for modal parameter estimation

Baker Bridge has been evaluated through a sequence of measurements using the IMUs in particular:

- On 6th February 2015 the bridge was visited by researchers for a short 'preliminary test' of bridge ambient vibrations under normal operating conditions enhanced a little by researchers walking up and down;
- On 26th February (along with pedestrian walking tests for the student project) and then on 11th June 2015 jumping tests were used to provide forcing functions and response data for point mobility estimation and then, via mode shapes, to estimate modal mass.

These tests are described in sequence, focusing on the use of IMUs for modal testing with and without artificial excitation (by jumping).



Fig. 3. Baker Bridge.

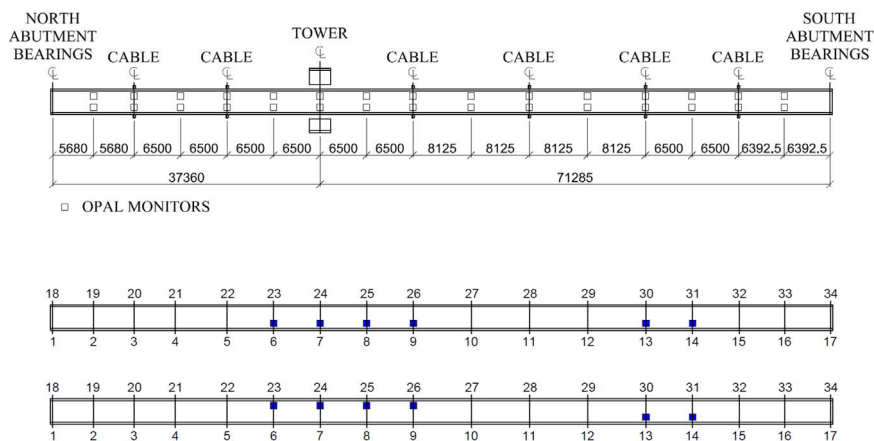


Fig. 4. Locations of measurement/test points (TPs), and TPs used for two of the seven five-minute recordings.

#### 4.1. Ambient vibration testing (AVT) with IMUs for mode shape and frequency estimates

In preparation for pedestrian tests to be carried out on February 26th and to provide mode shapes for modal mass estimation, ambient vibration measurements were made on Baker Bridge on the afternoon of 6<sup>th</sup> February 2015 during which time there was little pedestrian traffic (Fig. 3).

Before travelling to the bridge the set of six (Opal<sup>TM</sup>) IMUs was set to acquire signals in the *synchronised logging* mode and 2 g range, undocked from the base station and put in a jacket pocket for the short drive to the bridge. At the bridge a grid of 34 test points (TPs) indicated in Fig. 4 was marked out using a tape measure and chalk. Four TPs were at abutments where vertical motion was assumed to be zero. The IMUs were then 'roved' over 30 TPs in seven recordings as follows.

Two IMUs were kept at the same two reference TPs. TP13 and TP14 were chosen based on intuition that the front span would participate in most of the response, and that the first six modes of interest would be unlikely to have nodes (zero motion) so close to the south abutment. The remaining four IMUs were moved to TP1, TP2, TP3, TP4 and left for five minutes before moving them to four more TPs and so on in a sequence of seven recordings.

IMU locations for two recordings respectively having IMUs at TP13, TP14, TP23, TP24, TP25, TP26 (recording three) and TP13, TP14, TP6, TP7, TP8, TP9 (recording four) are indicated in Fig. 4. For all recordings IMUs were taped to the bridge to prevent being accidentally kicked off the walkway. In this way each TP would have a vibration measurement synchronous with two reference points, allowing for mode shapes to be assembled. After marking out the grid, the whole exercise including gaps in the measurement sequence while moving IMUs took 67 min.

After return from site and docking IMUs to the base station, data were downloaded, split time-wise into a sequence of seven five-minute recordings and analysed using the NExT/ERA operational modal analysis procedure [18]. This is one of many possible operational modal analysis procedures [e.g. 19,20] and was used here due to long experience in its use and implementation in bespoke software [21].

Only the vertical acceleration signals from the seven five-minute recordings were used since the bridge exhibited no significant lateral vibrations, and each of these seven recordings was truncated to 256 s as two consecutive 128 s frames.

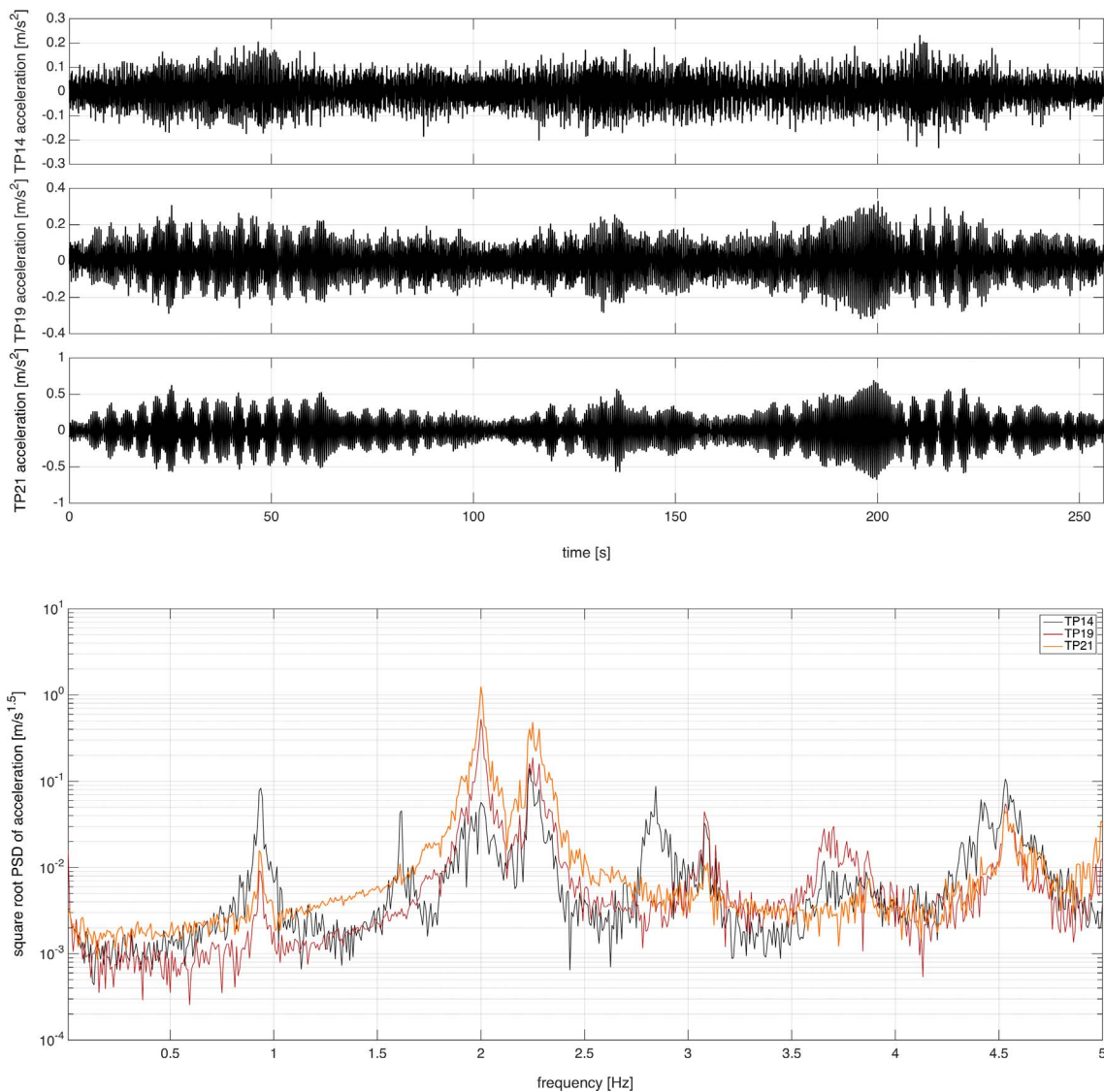


**Fig. 5.** Acceleration time series measured at TP14, TP19 and TP21 (top three plots) and their corresponding square-root power spectral densities (bottom plot), for recording 1.

6 × 6 Cross-spectral density (CSD) matrices were created from these without overlap or windowing, normalised with respect to the reference sensors and merged into a single 30 × 2 CSD matrix. Fig. 5 shows time series and auto-spectra for recording 1.

The CSD matrix was truncated to 8 Hz then transformed to time domain as impulse response functions (IRFs) for the ERA procedure. Based on this, a set of six apparent modes is visible up to 3.5 Hz, although only TP14 shows any response around 1.6 Hz in Fig. 5. Inspection of time-frequency data (spectrogram) suggests the beating phenomenon clear at TP21 might be due to two close modes around 2 Hz. The NExT/ERA procedure produced a remarkably clean set of modes, which are presented in Fig. 6. Mode 2 as identified does not appear to be purely vertical, and Mode 5 is almost pure torsion, with very little lateral movement. The mode shapes indicated for 2 Hz and 2.24 Hz are almost identical except for phase angle of the back span, and explain the beating observed in the time series (Fig. 5).

The aim of the AVT was to estimate mode shapes and frequencies for scheming the subsequent measurements that would include jumping and hammer tests at suitable nodes identified in this preliminary test. It is well known that parameter estimates from operational modal analysis carry significant uncertainty, particularly for damping. Recently developed uncertainty laws [22] were applied assuming the estimates from Fig. 6 as most probable values so that for mode 1 the recording duration is 240 times the natural period. The standard error (standard deviation/most probable value) takes a minimum of 0.0015 for frequency and 0.45 for damping. Although these are upper bounds, the frequency estimates and the mode shapes are sufficiently reliable to fulfil the requirement of guiding the subsequent testing in which more precise

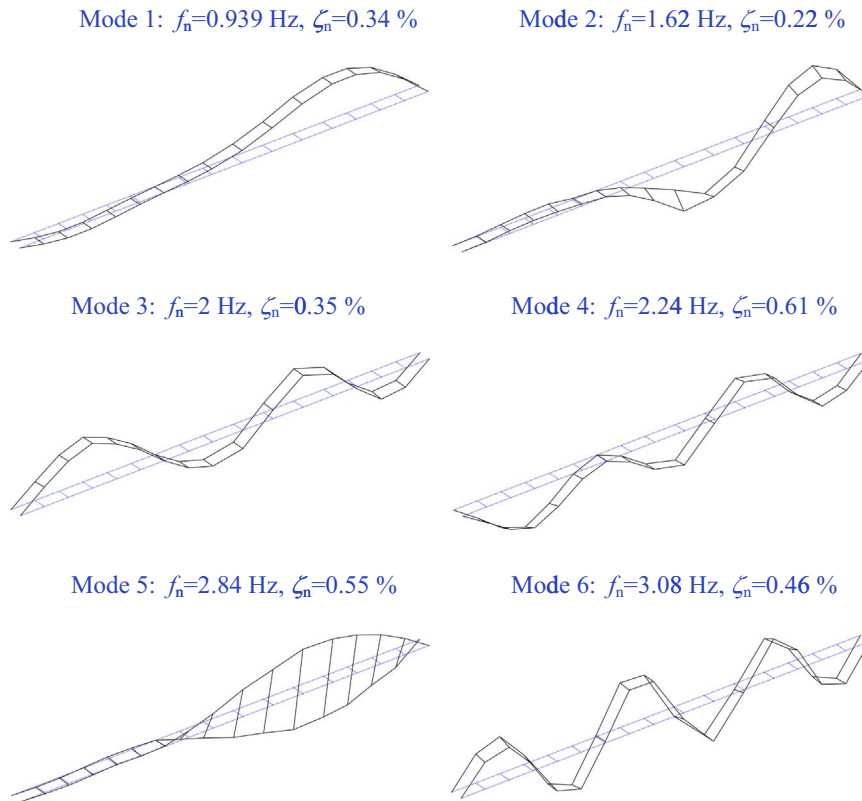


Fig. 6. Mode shapes and frequency estimates from preliminary test. Longer front span is to the right in each mode.

estimates of frequency and damping were obtained using the traditional method of logarithmic decrement applied to vibration free decay.

#### 4.2. Jumping tests for modal mass estimation

Jumping tests were used to generate forces that could be measured using IMUs on two occasions, first during the pedestrian testing without a force plate and using an ‘instrumented student’, then in a separate test taking a force plate to provide on-site calibration and corroboration with results from a different instrumented researcher.

Fig. 7 shows the ‘instrumented student’ (5<sup>th</sup> author) preparing for a laboratory trial before going to Baker Bridge.

The signals in Fig. 8 are an example for jumping on the bridge at TP13 (Fig. 4) to excite the first mode. The force data in Fig. 8(a) are simply the vertical acceleration of the sternum IMU scaled by the student mass (74 kg). This simple approach was expected to provide a rather crude representation – using a single strategically placed IMU, but it turned out to be surprisingly reliable for the purpose.

We have discovered [10] that the best approach to generate large amplitude response is to jump between four and eight times at a rate corresponding to a reasonable estimate of the natural frequency and then stop. Because the jumping rate might not exactly match the natural frequency and because the natural frequency may change as amplitude increases, there comes a point when further jumping reduces response or at least the exponentially asymptotic build-up of vibration amplitude is not sustained.

Hence, prompted by a metronome set to 54 beats per minute (bpm), the student jumped five times and then stood perfectly still for the remaining (approximately) 65 s. 54 bpm corresponds to a frequency of 0.9 Hz, the approximate first natural frequency of the bridge (see Fig. 5). Fig. 8(b) shows the corresponding acceleration response at TP13.

Force/response data such as these can be analysed applying traditional frequency domain identification techniques, e.g. circle fit or global rational fraction polynomial (GRFP). Both these methods operate on the frequency response function (FRF)  $\alpha_{j,k}(\omega)$  which in the form of a receptance function is the frequency domain ratio of displacement response at point  $j$ ,  $X_j(\omega)$ , to forcing function at point  $k$ ,  $F_k(\omega)$ , obtained via FFT of force and response time series:

$${}^n\alpha_{j,k} = \frac{X_j(\omega)}{F_k(\omega)} = \frac{1}{m_n} \cdot \frac{{}^n\psi_j {}^n\psi_k}{\omega_n^2 - \omega^2 + 2i\zeta_n\omega_n\omega} \quad (1)$$





Fig. 7. Instrumenting a student with IMU on sternum (circled), and lower back.

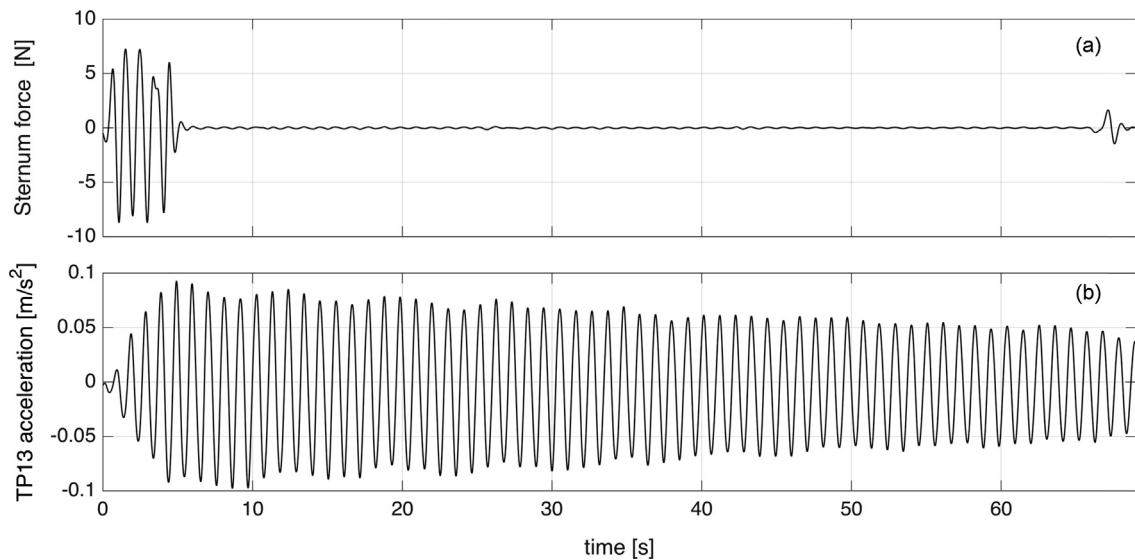


Fig. 8. Results of jumping test: (a) Estimated jumping force at TP13, via IMU attached to sternum of 74 kg student (Fig. 7) jumping at 54 jumps per minute, (b) acceleration response at TP13.

Via Eq. (1) a modal constant  ${}^n A_{j,k}$  is defined as

$${}^n A_{j,k} = \frac{{}^n \psi_j {}^n \psi_k}{m_n}. \quad (2)$$

For mode  $n$ ,  ${}^n\psi_j$  is the modal ordinate at test point  $j$ ,  $(\omega)_n$  is the circular natural frequency equal to  $2\pi f_n$ , where  $f_n$  is the natural frequency,  $\zeta_n$  is the modal damping ratio and  $m_n$  is the modal mass. If  $j=k$  then the FRF represents 'point mobility'. If point  $j=k$  has the largest modal ordinate and if this is set to unity value, i.e.  ${}^n\psi_j = {}^n\psi_k = 1.0$ , then modal mass is the reciprocal of the modal constant.

FRF curve fitting requires good resolution in frequency domain around the modal peaks. A measure of this resolution is the number of frequency lines  $n_{\text{HPB}}$  between points where FRF is 70 percent of maximum value, which mark the so-called 'half-power' band (hence HPB subscript in  $n_{\text{HPB}}$ ) and is determined as

$$n_{\text{HPB}} = 2\zeta_n f_n / df. \quad (3)$$

The frequency spacing  $df$  is the inverse of the duration  $T$  of the transient event and with very low damping  $n_{\text{HPB}}$  may correspond to less than one spectral line, providing very poor frequency domain resolution of the resonance curve.

To improve the frequency domain resolution and offer more points to fit around the sharply changing resonance function, exponential time window

$$W(t) = e^{-\beta t/T} \quad (4)$$

is applied, introducing adding damping

$$\zeta_{n,\text{add}} = \beta / (\omega_n T). \quad (5)$$

For this example with  $T = 69$  s and  $f_n = 0.93$  Hz,  $\omega_n = 10.18$  rad/s and  $\zeta_n = 0.22$  percent (estimate from NExT/ERA),  $n_{\text{HPB}} = 0.5$  and  $2.7$  respectively without and with added damping  $\zeta_{n,\text{add}} = 0.99$  percent, for  $\beta = 4$ . Beta was chosen such as to assure that the exponential window decays to below 2 percent of its initial value (unity for  $t=0$  in Eq. (4)) at the end of the record thus reducing the effect of leakage.

The classical circle fit method [23] was chosen for modal parameter estimation because the Nyquist plot of real and imaginary components of the receptance FRF  $\alpha_{j,k}(\omega)$  appears as a circle allowing clear visual interpretation of modal properties. Strictly speaking it will be a perfect circle only for hysteretic damping whereas the mobility FRF (the ratio of velocity to force) is a perfect circle for viscous damping. In practice inertance FRF is actually measured, as the ratio of acceleration to force. At (circular) frequency  $\omega$  inertance takes values  $-\alpha\omega^2$  and still maps to an almost perfect circle.

The inertance FRF resulting from the data of Fig. 8 after applying the windowing function of Eq. (4) is represented as the diamond data points in Fig. 9, and the smooth circle represents the best fit to the data. For the inertance FRF the circle diameter  $D$  is proportional to the modal constant via

$${}^n A_{j,k} = 2\zeta_n D / \omega_n^2. \quad (6)$$

The natural frequency  $\omega_n$  is found where the rate of change of phase angle with respect to frequency is greatest and the damping is found from that rate of change of phase. The added damping due to the exponential window provides more points to define the circle but does not affect the estimate of the modal constant which yields a modal mass of 55.5 t.

To cross-check this value (55.5 t) and an estimate of 49.9 t obtained using the jumping force estimated using a single IMU on the lower back, the modal mass (for mode 1) was also estimated using the mode shape (see Fig. 6) and the mass distribution obtained from the structural drawings, summing mass assumed lumped at each TP scaled by squared modal ordinate at the TP i.e.

$$m_n = \sum_j {}^n\psi_j^2 m_j. \quad (7)$$

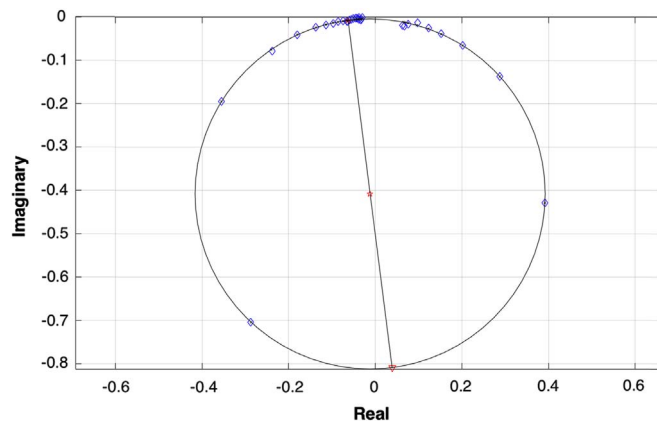


**Fig. 9.** Circle fit (for mode 1) to frequency response function between acceleration response and jumping force reconstructed based on sternum data for TP13 shown in Fig. 8. Units are  $\text{ms}^{-2} \text{kN}^{-1}$  and the resulting modal constant is  $1.802 \times 10^{-5} \text{kg}^{-1}$ . Modal parameter estimates are:  $m_1 = 55.5$  t,  $f_n = 0.936$  Hz,  $\zeta_1 = 1.11$  percent (before correction).

$m_j$  is the mass of the bridge assumed lumped at test point  $j$  which can be estimated as the mass of the length of deck centred halfway to the adjacent test points in opposite directions along the deck. This estimate is referred to as 'mass sum' in this paper.

Considering only the deck mass in the summation (the pylon movement was not measured) gives an estimate of 37 t, suggesting either an error in the circle fit or that other massive parts of the bridge (e.g. pylon) are strongly engaged in the mode.

Circle fit is just one of several modal analysis techniques available and is best suited to well separated modes, but it provides a clear graphical indication of the quality of the fit. However, a better estimate of the frequency and damping can be obtained when a clear single mode free decay response is available. A bandpass filter (0.5 Hz to 1.3 Hz) was applied to the response data of Fig. 8(b) to remove low frequency drift and any response of higher vibration modes. Next an exponentially decaying sine wave was fitted to the time series, providing frequency and damping estimates of 0.937 Hz and 0.16 percent respectively for mode 1. The damping corresponds to the response levels generated during the jumping and is assumed to be constant whereas both damping and frequency are typically amplitude-dependent [24].

Although data from the sequence of jumping at different rates were recorded, their value was limited by the short interval between jumping sequences allowed by the test schedule. This affected the frequency resolution for the circle fitting and also did not allow sufficient time for the signals to decay to levels not affecting subsequent jumping response.

This is a negative aspect of using IMUs in *synchronised logging* mode: the response cannot be viewed in real time, it can only be examined from downloaded data. On-site download and inspection was not feasible in this case, but the experience was useful for designing additional jumping tests to estimate masses for other modes.

#### 4.3. Jumping tests using force plate and IMU at C7 vertebrae

Provided the point where the IMU is attached to the body is such that it accurately captures the acceleration of the centre of mass, the simple product of body mass and IMU vertical acceleration can apparently provide a reliable estimate of the ground reaction force (GRF). Then all that is required is acceleration data from two IMUs (one on the body, and one on the footbridge) and a knowledge of modal ordinates. So far, it has not been certain which is the best position on the human body to capture with best accuracy the GRF. Hence further measurements were made using additional body measurement points and also using a long time interval between jumping sequences to allow good frequency resolution. Also to provide a one-time direct check, an AMTI Optima 464508-1000 force plate was taken to site, on 11th June 2015.

One set of six IMUs was set at test points on the South end of the front span, and a second set was used to instrument 2<sup>nd</sup> author with IMUs on right foot, lower back, sternum, navel using mounting straps and also with one attached to the C7 vertebra on the back of the neck using double-sided medical grade adhesive tape, making 11 IMUs in total.

All 11 IMUs operating in synchronised logging mode were assembled into a single network to maintain the same notion of time. The force plate data, sampled at 1000 Hz, were downsampled to the sampling frequency of IMUs (128 Hz) using an antialiasing finite impulse response filter, compensating for the delay introduced by the filter. To align time series for IMUs with a force plate, a single jump was recorded and the time axes were slid such as to achieve maximum correlation coefficient between the similar-shape signals.

Fig. 10 shows the experimental setup used with the 2<sup>nd</sup> author jumping on the force plate, which was taken to site to provide a validation of the procedure. Foot, sternum and navel IMUs are visible but unfortunately either partially obstructed by or not contrasting well with the clothing, so IMUs are shown circled in red in the figure. The force plate is located at the transverse centre of the bridge between TP4 and TP21 (Fig. 4) which is an antinode of mode 3.

The data from the force plate were corrected for the inertia force of the 28 kg self-mass using the bridge acceleration signal and compared with forces reconstructed from three IMU sensors ('C7', 'Sternum' and 'Lower back'). Fig. 11(a) shows the comparison of GRF time histories measured directly using the 'force plate' with reconstructed values for sternum, lower back and C7 vertebra. It can be seen that the GRFs reconstructed using sternum and lower back accelerations overestimate the directly measured force significantly during the impact phase of the jump, while reconstruction using acceleration from the C7 vertebra (on the back of the neck) shows good agreement with the force plate data.

To examine how the force signals compare in the frequency domain, Fig. 11(b) shows the FFTs of the whole duration of the signals partially shown in Fig. 11(a). It can be seen that up to about 3.5 Hz there is good agreement between all the components of reconstructed force, while there are noticeable differences in the components of force around the second harmonic of the jumping frequency (4 Hz), with the ordinates of the C7 data being closest to those of the force plate data.

Fig. 11(c) shows the linear build-up of response that justified the modal mass estimation method proposed in [10].

#### 4.4. Investigation on reliability of IMU data for force estimation

So far only two test subjects were used, which may not be representative. Therefore a dedicated experimental campaign was conducted on a rigid laboratory floor to obtain a small database of directly measured GRFs and IMU data. The force plate was located on a flat surface and seven subjects (jumpers) aged 25 to 57 were tested, including two females and five males, weighing from 54 kg to 104 kg. Each subject was asked to jump for 20 s at each of nine frequencies from 1.5 to 2.1 Hz, in 0.1 Hz increments and at 2.25 Hz and 2.4 Hz, the last two corresponding to two bridge mode frequencies. Therefore in total sixty-three tests were conducted giving twenty-one minutes of jumping time. Each subject was instrumented with an IMU at C7, lower back (LB) and sternum (S). IMU and force plate signals were acquired separately and aligned in a post-processing phase, as explained in Section 4.3.

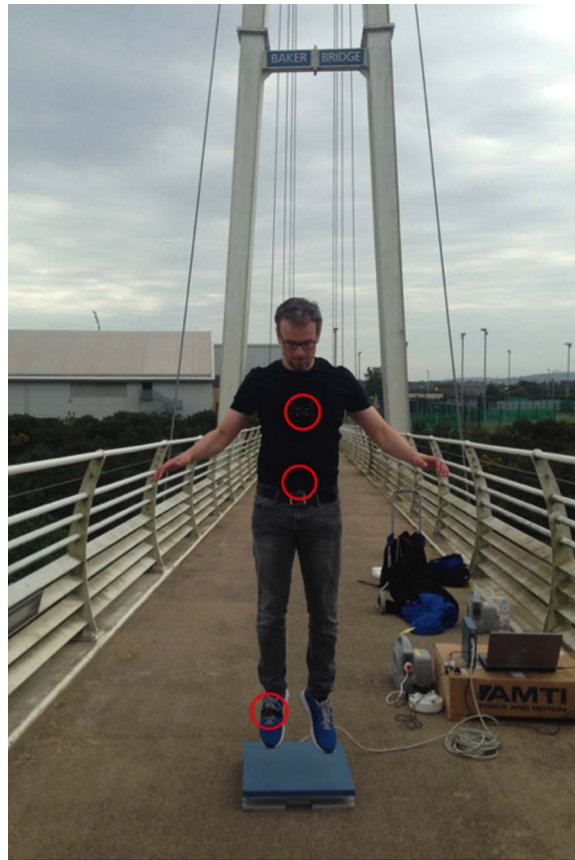


**Fig. 10.** Jumping test at Baker Bridge. Second author is instrumented with IMUs at sternum, navel, lower back and C7 (not visible) and right foot; the bridge is instrumented with IMUs and a force plate. The collection of equipment around the cardboard box is necessary to operate the force plate.

For each sequence the largest number of complete jumps was identified from force plate signals to obtain the best resolution of data in the frequency domain. In order to avoid leakage in spectral calculations, the signals were truncated to include an integer number of jumping cycles based on threshold detection.

Jumping sequences with clearly dominant FFT peaks were identified from which the ratios of FFT amplitudes of force reconstructed based on data from IMUs and directly measured by the force plate were obtained (as indicated on Fig. 11). Subject masses were estimated from differences of force plate signals with and without the subject standing (still) on the force plate, which was in turn calibrated with known weights. The comparison for 43 jumping sequences is presented in Fig. 12. The remaining 20 sequences were not useful as they demonstrate difficulty in keeping to a metronome beat, resulting in highly variable footfall timing, spreading of energy in frequency domain and multiple FFT peaks. The size of the marker is proportional to the dynamic load factor (DLF) that is the magnitude of the harmonic force component expressed as a fraction of the weight of the walker or jumper. Marker size in the legend of Fig. 12 indicate unit value DLF.

The comparison only involves the fundamental component, and as Fig. 11 suggests, some of the jumping 'energy' could appear in higher harmonics. In the figure the ratios are based on single Fourier lines, but due to the good correspondence of directly and indirectly measured forces in the frequency domain the single line values are reliable and are almost identical to ratios reflecting signal strengths over narrow frequency bands around the harmonic peaks. These ratios were obtained as the square root of power spectral densities integrated from 5 percent below to 5 percent above the frequencies for peak signal strength. The average ratio of DLFs computed using the power spectral densities to those obtained for a single line, and with weighting by the DLF, is 1.04 with standard deviation 0.04 for C7. Hence when using C7 acceleration to estimate modal mass, the value should be adjusted down by 4 percent.

The evidence is clear: IMU data will slightly overestimate force (and hence mass) and data for single IMUs at either C7 or lower back signals could be used, with C7 preferable due to lower scatter.

#### 4.5. Summary of modal mass estimation

The mass and damping estimated for modes 1–4 (the ones most strongly excited by pedestrians) are summarised in Table 1, with adjustment of IMU-derived GRFs based on Fig. 12. Estimates are provided using force estimates from IMU-derived GRFs, for hammer testing (unsuccessful for mode 1), for direct measurement using force plate (not tried for mode 1) and for mass sum based on mode shape ordinates and structural data. These last values seem to be very much out of line

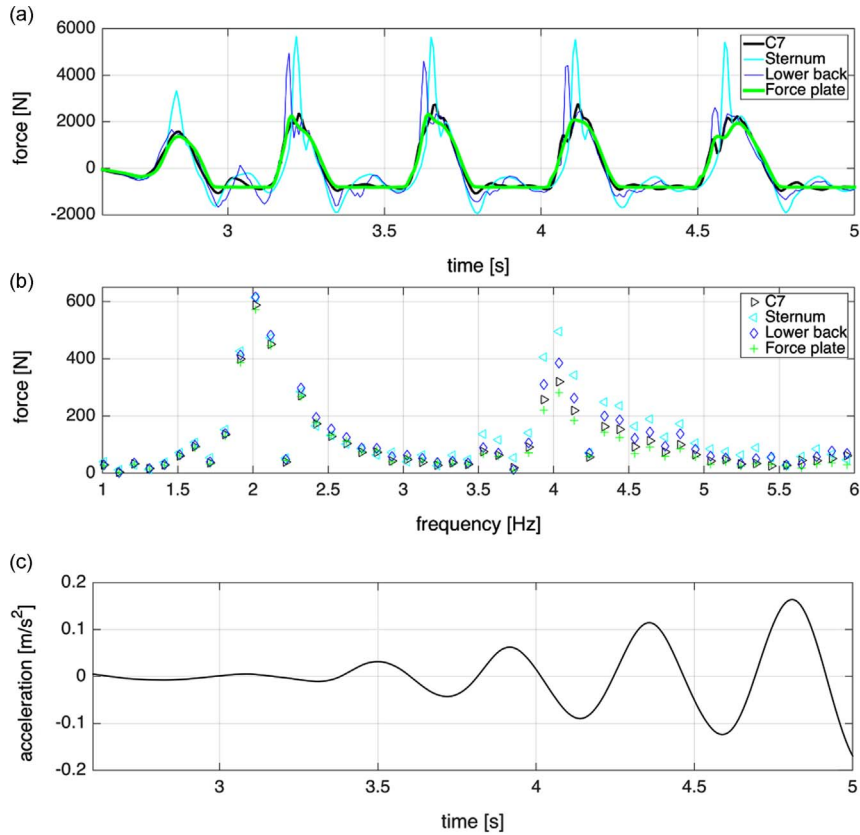


**Fig. 11.** Jumping forces from force plate (measured directly) and Opal™ IMUs (measured indirectly) for the second author jumping at 2 Hz between TP4 and TP21: (a) Time series, (b) Fourier line amplitudes of 10 s duration force signals of which truncated time histories are shown in (a), (c) growing deck acceleration response.

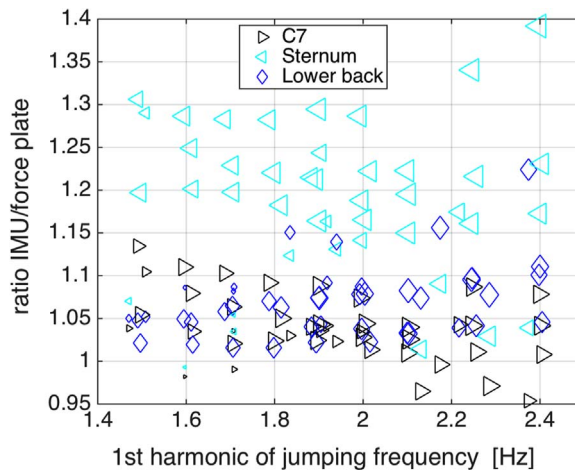


**Fig. 12.** Reliability of IMU force data for first harmonic of jumping frequency. Marker size indicates DLF, markers in legend are for unit value DLF.

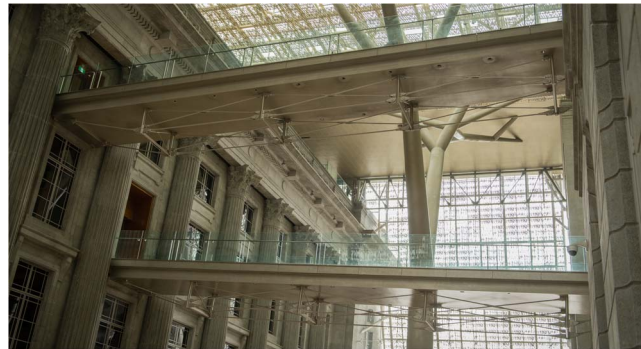
with the experimental estimates. This marked difference has been observed on other structures and experience shows that the experimental estimates should be used. In this case it is most likely that other massive parts of the bridge (e.g. pylon) are also engaged in the modes examined.

Few data are available for mode 1 because the natural frequency is below the dominant frequency of typical pedestrian loading and this mode is much less responsive to pedestrian forces than modes 2, 3 and 4, on which the exercise was primarily focused, hence Fig. 9 represents the only data defining mode 1.

**Table 1**

Modal mass and damping estimate summary.

Force from	Mode 1 $f_n = 0.94$ Hz		Mode 2 $f_n = 1.61$ Hz		Mode 3 $f_n = 2.00$ Hz		Mode 4 $f_n = 2.24$ Hz	
	$m_n$ [t]	$\zeta_n$ [%]	$m_n$ [t]	$\zeta_n$ [%]	$m_n$ [t]	$\zeta_n$ [%]	$m_n$ [t]	$\zeta_n$ [%]
C7	n/a	n/a	74.8	0.18	60.6	0.29	59.9	0.36
Sternum	55.5	0.16	84.5	0.18	65.9	0.28	65.5	0.35
Lower back	49.9	0.17	75.8	0.18	64.5	0.28	63	0.37
Force plate	n/a	n/a	68.4	0.19	57.2	0.32	57.3	0.37
Mass sum	37	0.48	34	0.20	40	0.30	42	0.26
Hammer	n/a	n/a	n/a	n/a	57.5	n/a	n/a	n/a

**Fig. 13.** Skybridges at National Gallery, Singapore. SB4 is the upper bridge.

For modes 2–4 the closest estimate to the force plate-derived mass estimate is for C7 data, for which no measurement was available for mode 1. For mode 3 a single result using an instrumented hammer during the student test is reported for comparison. The result for mode 3 is the clearest among attempts to identify modes from hammer test circle fit data which were limited by the short interval between hammer impacts. There is also a slight worry with having to rely on the hammer load cell original calibration data or (for such a large hammer) a non-trivial recalibration exercise. The advantage of using jumping forces is direct calibration of accelerometers against gravity (inverting accelerometers) and the force plate against standard calibrated weights.

Assuming reliable instrument calibration, both the hammer and the force plate estimates resulting from direct measurement of force would be expected to give similar modal mass estimates, and this is indeed the case. Using force plate data and hammer data the modal mass for mode 3 was calculated to be 57.2 t and 57.5 t, respectively.

## 5. Demonstrating the value of the methodology

Even before the well-publicised vibration serviceability failure of the London Millennium Footbridge [2] footbridge vibrations have been a serviceability issue [25,26]. With introduction of more sophisticated vibration serviceability standards, greater awareness of the issue and enhanced concern about public complaints arising from the performance of high-profile structures, modal testing and pedestrian load tests before opening to public use are an effective way to reduce risk.

In such high profile structures reliable modal identification is required, traditionally using some form of shaker. For example, vibration testing of the London Millennium Bridge [27] used step-sine testing with a purpose-designed reciprocating mass hydraulically driven shaker for lateral force generation and a rotating eccentric mass shaker for vertical force generation. With technology advances, the standard test procedure now involves electro-dynamic shakers capable of providing broadband random excitation. Testing of the Singapore Helix Bridge [3] employed two such shakers to identify the modal properties which were subsequently used for simulation of dynamic response to crowds jumping or walking. The shakers were borrowed locally to avoid costs of airfreighting over 150 kg of equipment, but the accelerometers, data acquisition systems and peripheral equipment still had to be airfreighted, with significant costs and delays with customs clearance.

A request from National Gallery Singapore to evaluate the vibration serviceability of a footbridge provided an opportunity to prove the capability of the IMU-based modal testing procedure. The measurements relied on nothing more than two sets of Opal™ IMUs, carried by the test team as aircraft hold baggage along with a backup set of four conventional wired accelerometers and a compact USB data acquisition system.



Fig. 14. Jumping on Skybridge SB4 with IMUs attached to jumper C7 and deck at midspan.

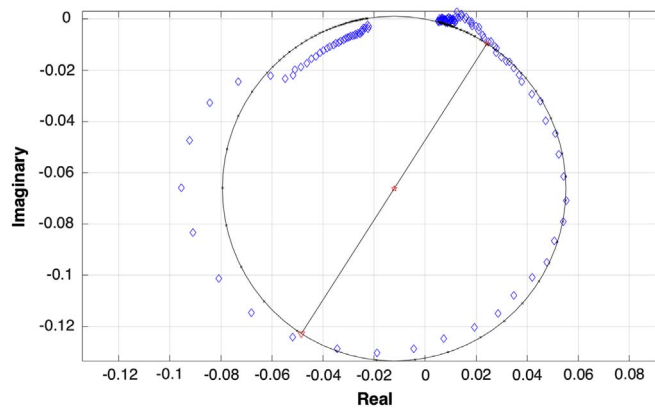


Fig. 15. Circle fit (for mode 1) to frequency response function between bridge midspan acceleration and C7 vertical acceleration for Skybridge SB4. The plot is dimensionless and the modal constant is 0.0058. Modal parameter estimates are:  $f_n = 4.023$  Hz,  $\zeta_1 = 2.17$  percent.

The studied footbridge is the upper of the two ‘Skybridges’ shown in Fig. 13 and spanning a 21.2 m wide atrium between Singapore’s former Supreme Court and City Hall buildings. It comprises two  $2 \times \text{UB } 457 \times 191 \times 98 \text{ kg m}^{-1}$  steel main chords supporting secondary steel cross beams,  $3000 \times 125 \text{ mm}$  reinforced concrete on 1 mm Bondek, with 20 mm concrete topping forming the deck, and Macalloy bar trusses and cross-bracing to increase stiffness for vertical vibrations. Due to the national significance of the new museum, opened in November 2015, the bridge was investigated to confirm vibration serviceability to appropriate standards, including an estimation of modal properties in the unlikely event that retrofit needed to be considered.

With a preliminary estimate of 4 Hz natural frequency obtained during a reconnaissance visit in September 2015, jumping at 2 Hz (Fig. 14) was used to excite response via the second harmonic, which was not investigated in the Baker Bridge study.

Mode shapes were identified by IMU measurement of ambient vibrations and vibrations generated by jumping and walking activities. The frequency response function between C7 acceleration (proportional to jumping force) and bridge acceleration response is given in the form of a Nyquist plot in Fig. 15 for the lowest mode with approximate natural frequency 4 Hz. To obtain the modal constant and hence modal mass requires scaling by the mass of the jumper and application of a correction factor such as shown in Fig. 12 for second harmonic frequency of jumping.

The simple assumption that C7 acceleration scaled directly by body mass provides the GRF was checked using the same laboratory data set and methodology represented in Fig. 12, but for the second harmonic frequency of jumping. The correspondence of GRF estimates from jumper mass for different IMU locations with GRFs measured directly with the force plates is shown in Fig. 16. With weighting by the DLF, the average ratio for C7 is 1.135 with standard deviation 0.175, hence body mass reduced by 13.5 percent should be used for modal mass estimation using second harmonic frequency of jumping.

The modal constant from the circle fit to the FRF in Fig. 15 for the 81 kg 2<sup>nd</sup> author jumping on SB4, after adjusting the IMU-generated GRFs by 13.5 percent, provides an estimate of  $81/(1.135 \times 0.0058) = 12.3 \text{ t}$ . As a cross-check on modal mass, summing mass distribution according to the stated structural values and scaling by (squared) measured unity-scaled mode shape ordinates provides an estimate of 13.15 t.

Skybridge response data measured by IMUs (not reported here) demonstrated acceptable vibration serviceability so there was in this case no need to use the modal parameter information to design mitigation measures. The lower of the two footbridges shown in Fig. 13 was also studied, but having a higher natural frequency it exhibited even better response to pedestrian loading.

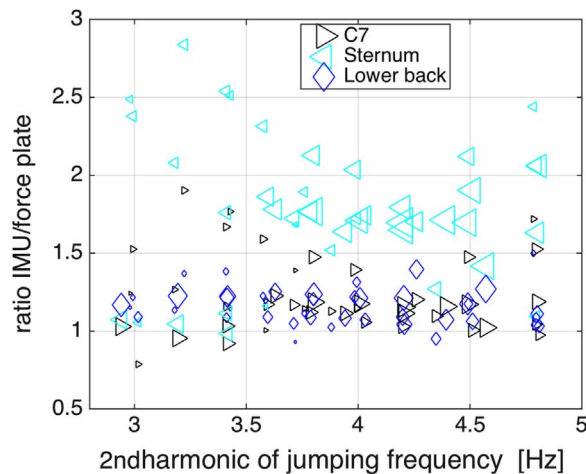


Fig. 16. Reliability of IMU force data for second harmonic of jumping frequency. Marker size indicates DLF, markers in legend are for unit value DLF.

## 6. Summary

The story presented in this paper tracks the development of a procedure for using IMUs developed for the biomechanics market for the rather different application of footbridge modal testing. What began as a student project using the IMUs to study pedestrian synchronisation and its effects on vibration serviceability of footbridges took a side track to efficient parameter estimation in a sequence of experiments spanning a year. The activities undertaken and main findings are summarised here for the benefit of the reader.

The first measurements (February 6th 2015) were intended to aid the student study of synchronisation on 26<sup>th</sup> February but to our surprise it proved an excellent data set for operational modal analysis. Due to the tight timing of the student study, only a very limited range of tests on jumping-induced response was possible. By then it was not known that C7 was the best location for an IMU, yet this limited testing was able to provide an excellent estimate of first mode parameters. In the same exercise a brief hammer test was conducted providing an estimate of the third mode mass and highlighting the difficulty in using this type of excitation, leading us to concentrate on the jumping tests. There followed an exercise in March 2015 (not reported) to further explore the capability, and the definitive test on 11<sup>th</sup> June in which C7 was used, the force plate was taken to site as a cross-check, and the modal properties of second, third and fourth modes were estimated. In August the exercise with nine subjects jumping on the force plate while instrumented with IMUs was used to compare directly and indirectly obtained forces thus calibrating the force reconstruction method.

The opportunity to apply the technique on the Skybridge materialised in late August 2015 and after the natural frequency was checked during a brief visit to Singapore in September, the August force plate/IMU data were revisited to check for ability of IMUs to estimate forces at the second harmonic frequency of jumping. Having confidence that the method would work, it was applied for parameter estimation during the Skybridge testing on 6th November 2015. Being a commercial test which could not fail, conventional instrumentation was used as backup for data acquisition only, there being no further local access to shakers used for the Helix Bridge [3]. In fact it turned out the whole test, including a large set of response measurements (that it would not be possible to report on here) could have been carried out using a pocketful of IMUs, a laptop and IMU docking station.

## 7. Conclusions

The paper describes the use of inertial measurement units (IMUs) for motion capture to identify ground reaction forces (GRFs) as well as for ambient vibration testing of footbridges in field conditions. All that is required for this process is a set of compact wearable wireless sensors, with the C7 (neck) vertebra being the most suitable IMU location for estimating GRFs. This appears to be the first exercise proving this capability allowing for simple and reliable field estimation of modal mass.

The methodology was demonstrated using data from a cable-stayed footbridge in Exeter having frequencies around the first harmonic frequency of jumping, and the technique was subsequently applied to a simply supported footbridge in Singapore having natural frequency in the range of second harmonic frequency of normal jumping. In both cases modal mass estimates were corroborated by independent methods.

While it is possible for the IMUs used to stream data in real time when operated in close proximity to the wireless access point, the IMUs were operated in a *synchronised logging* mode for both bridge tests. This mode does not allow for checking data in real time but this did not compromise the testing while allowing for remarkable logistical simplicity.



The developed procedure could prove useful for testing footbridges for which modal frequencies fall within the range of frequencies for the first and second harmonics of feasible jumping, which are likely to suffer from vibration serviceability problems.

## Acknowledgements

The research was supported by EPSRC (grant reference EP/I029567/2), was possible via permission of Devon County Council and was assisted in the UK and Singapore by James Bassitt.

## References

- [1] P. Dziuba, G. Grillaud, O. Flamand, S. Sanquier, Y. Tetard, La passerelle Solferino: Comportement dynamique (Solferino bridge: Dynamic behaviour), *Bulletin Ouvrages Métalliques* (2001) 34–57.
- [2] P.R. Dallard, A. Fitzpatrick, A. Flint, A. Low, R. Ridsdill Smith, *The Millennium bridge, London: problems and solutions*, *Structural Engineer* 79, 2001, 15–17.
- [3] J.M.W. Brownjohn, P. Reynolds, P. Fok, Vibration serviceability of Helix Bridge, Singapore, *Proceedings of the Institution of Civil Engineers: Structures and Buildings* 169 (8) (2016) 611–624.
- [4] E. Caetano, A. Cunha, F. Magalhães, C. Moutinho, Studies for controlling human-induced vibration of the Pedro e Inês footbridge, Portugal. Part 1: assessment of dynamic behaviour, *Engineering Structures* 32 (2010) 1069–1081, <http://dx.doi.org/10.1016/j.engstruct.2009.12.034>.
- [5] S.-I. Nakamura, T. Kawasaki, Lateral vibration of footbridges by synchronous walking, *Journal of Constructional Steel Research* 62 (2006) 1148–1160, <http://dx.doi.org/10.1016/j.jcsr.2006.06.023>.
- [6] S. Živanović, A. Pavić, P. Reynolds, Modal testing and FE model tuning of a lively footbridge structure, *Engineering Structures* 28 (2006) 857–868, <http://dx.doi.org/10.1016/j.engstruct.2005.10.012>.
- [7] E. Reynnders, D. Degrauwe, G. De Roeck, F. Magalhães, E. Caetano, Combined experimental-operational modal testing of footbridges, *ASCE Journal of Engineering Mechanics* 136 (2010) 687–696, [http://dx.doi.org/10.1061/\(ASCE\)EM.1943-7889.0000119](http://dx.doi.org/10.1061/(ASCE)EM.1943-7889.0000119).
- [8] A. Cunha, E. Caetano, F. Magalhães, C. Moutinho, Recent perspectives in dynamic testing and monitoring of bridges, *Structural, Control Health Monitoring* 20 (2013) 853–877, <http://dx.doi.org/10.1002/stc.1516>.
- [9] M. Yoneda, Human walking vertical force and vertical vibration of pedestrian bridge induced by its higher components, *International Journal of Civil, Environmental, Structural, Construction and Architectural Engineering* 9 (9) (2015) 1165–1171.
- [10] J.M.W. Brownjohn, A. Pavić, Experimental methods for estimating modal mass in footbridges using human-induced dynamic excitation, *Engineering Structures* 29 (2007) 2833–2843, <http://dx.doi.org/10.1016/j.engstruct.2007.01.025>.
- [11] V. Racić, J.M.W. Brownjohn, A. Pavić, Reproduction and application of human bouncing and jumping forces from visual marker data, *Journal of Sound and Vibration* 329 (2010) 3397–3416, <http://dx.doi.org/10.1016/j.jsv.2010.02.021>.
- [12] V. Racić, A. Pavić, J.M.W. Brownjohn, Modern facilities for experimental measurement of dynamic loads induced by humans: A literature review, *Shock and Vibration* 19 (2012) 1–15, <http://dx.doi.org/10.3233/SAV-2012-0727>.
- [13] M. Bocian, J.M.W. Brownjohn, V. Racić, D. Hester, A. Quattrone, R. Monnickendam, A framework for experimental determination of localised vertical pedestrian forces on full-scale structures using wireless attitude and heading reference systems, *Journal of Sound and Vibration* 376 (2016) 217–243, <http://dx.doi.org/10.1016/j.jsv.2016.05.010>.
- [14] S. Cho, H. Jo, S. Jang, J. Park, H.-J. Jung, C.-B. Yun, B.F. Spencer, J.-W. Seo, Structural health monitoring of a cable-stayed bridge using wireless smart sensor technology: data analyses, *Smart Structures and Systems* 6 (2010) 461–480.
- [15] B.F. Spencer, Wireless smart sensor for monitoring civil infrastructure, in: *Proceedings of the 6th International Conference on Structural Health Monitoring of Intelligent Infrastructure*, Hong Kong, China (2013), pp. 116–134.
- [16] D. Zhu, Y. Wang, J.M.W. Brownjohn, Vibration testing of a steel girder bridge using cabled and wireless sensors, *Frontiers of Architecture and Civil Engineering in China* 5 (2011) 249–258, <http://dx.doi.org/10.1007/s11709-011-0113-y>.
- [17] J.M.W. Brownjohn, F. Magalhães, E. Caetano, A. Cunha, Ambient vibration re-testing and operational modal analysis of the Humber Bridge, *Engineering Structures* 32 (2010) 2003–2018, <http://dx.doi.org/10.1016/j.engstruct.2010.02.034>.
- [18] G.H. James III, T.G. Carne, J.P. Lauffer, The natural excitation technique (NExT) for modal parameter extraction from operating structures, *International Journal of Analytical and Experimental Modal Analysis* 10 (1995) 260–277.
- [19] C. Gentile, N. Gallino, Condition assessment and dynamic system identification of a historic suspension footbridge, *Structural Control and Health Monitoring* 15 (2008) 369–388, <http://dx.doi.org/10.1002/stc.251>.
- [20] K. Van Nimmen, P. Van den Broeck, P. Verbeke, C. Schauvliege, M. Mallié, L. Ney, G. de Roeck, Numerical and experimental analysis of the vibration serviceability of the Bears' Cage footbridge, *Structure and Infrastructure Engineering*. <http://dx.doi.org/10.1080/15732479.2016.1160133>.
- [21] J.M.W. Brownjohn, H. Hao, T.-C. Pan, *Assessment of structural condition of bridges by dynamic measurements*, Applied Research Report RG5/97, Nanyang Technological University, Singapore, 2001.
- [22] S.-K. Au, Uncertainty law in ambient modal identification – Part II: implication and field verification, *Mechanical Systems and Signal Processing* 48 (2014) 34–48, <http://dx.doi.org/10.1016/j.ymssp.2013.07.017>.
- [23] D.J. Ewins, *Modal Testing: Theory and Practice*, Research Studies Press Ltd, Baldock, Hertfordshire, England, 2000.
- [24] J.M.W. Brownjohn, N.F. Tao, Vibration excitation and control of a pedestrian walkway by individuals and crowds, *Shock and Vibration* 12 (2005) 333–347, <http://dx.doi.org/10.1155/2005/857247>.
- [25] J. Blanchard, B.L. Davies, J.W. Smith, Design criteria and analysis for dynamic loading of footbridges, in: *Proceeding of a Symposium on Dynamic Behaviour of Bridges at the Transport and Road Research Laboratory*, Report number: TRRL SR275, Crowthorne, Berkshire, UK (1977), 1–11.
- [26] J.E. Wheeler, Prediction and Control of Pedestrian-Induced Vibration in Footbridges, *ASCE Journal of the Structural Division* 108 (1982) 2045–2065.
- [27] A. Pavić, T. Armitage, T. Reynolds, J.R. Wright, Methodology for modal testing of the Millennium Bridge, London, *Proceedings of the Institution of Civil Engineers: Structures and Buildings* 152 (2002) 111–121, <http://dx.doi.org/10.1680/stbu.152.2.111.38966>.